Electronic Supplementary Material (ESI) for Journal of Materials Chemistry C.

Bi_2S_3 nanowire networks as electron acceptor layers in solution-processed hybrid solar cells

Luisa Whittaker-Brooks, Jia Gao, Anna K. Hailey, Conor R. Thomas, Nan Yao and Yueh-Lin Loo

Supporting Information:

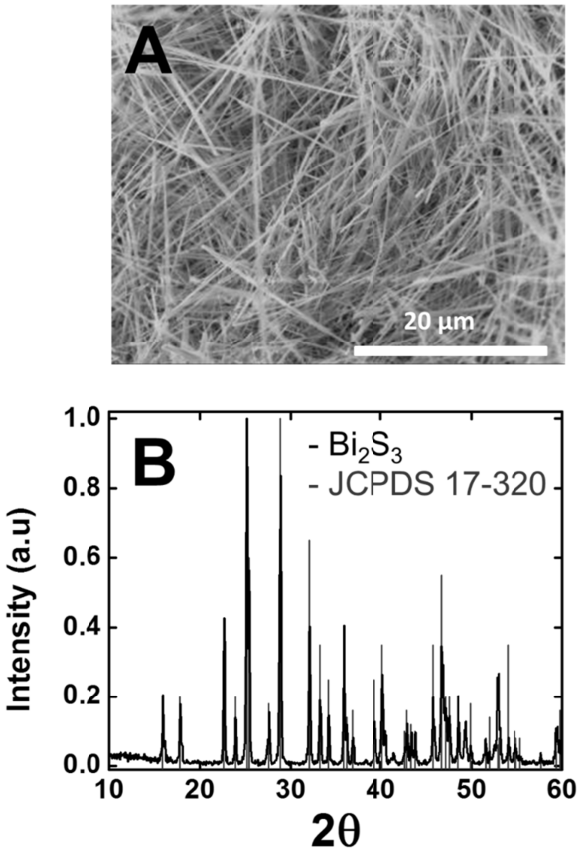

Figure S1. Structural characterization for Bi_2S_3 nanowires prepared by the hydrothermal reaction of $Bi(NO_3)_3$ and 2-mercaptoethanol. A) SEM image showing nanowires of Bi_2S_3. B) Powder diffraction pattern verifying the orthorhombic unit cell with *Pbnm* space group symmetry of as-synthesized Bi_2S_3 nanowires. Superimposed on the pattern is the identification of bulk Bi_2S_3, per JCPDS Card No. 17-320.

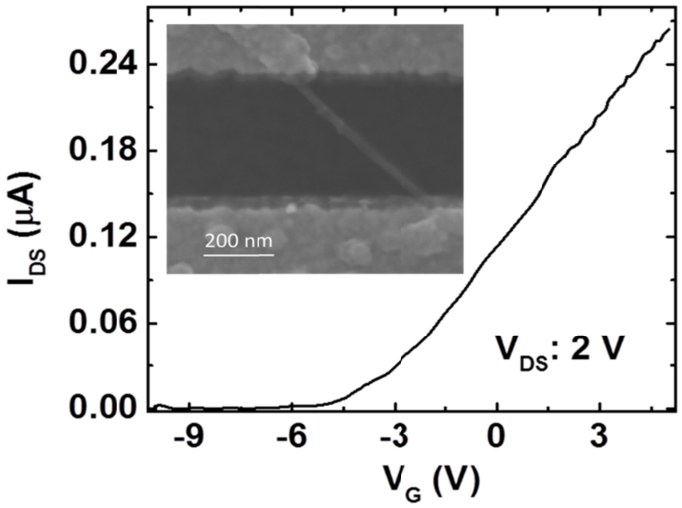

Figure S2. Transfer characteristics of a Bi_2S_3 single-nanowire field-effect transistor. Inset: SEM image of the channel region. The source and drain gold electrodes at the top and bottom of the image were defined by e-beam lithography and lift off; the nanowire is 30-nm in diameter.

Table S1. Device performance of hybrid solar cells comprising P3HT and percolated Bi_2S_3 networks with various thicknesses of both constituents.

Device batch[a]	Bi_2S_3 network thickness (nm)	P3HT thickness (nm)	J_{sc} (mA/cm^2)	V_{oc} (V)	FF	PCE (%)
1	50	120	2.7 ± 0.1	0.50 ± 0.07	0.34 ± 0.03	0.5 ± 0.15
2	140	120	7.7 ± 0.1	0.70 ± 0.05	0.43 ± 0.01	2.3 ± 0.02
3	200	120	10.7 ± 0.1	0.69 ± 0.01	0.45 ± 0.01	3.3 ± 0.01
4	240	120	4.2 ± 0.2	0.50 ± 0.08	0.40 ± 0.05	0.8 ± 0.10
5	200	100	9.6 ± 0.1	0.70 ± 0.01	0.40 ± 0.02	2.7 ± 0.02
6	200	180	9.7 ± 0.1	0.56 ± 0.03	0.33 ± 0.04	1.8 ± 0.03
7	200	200	5.7 ± 0.1	0.62 ± 0.02	0.41 ± 0.08	1.4 ± 0.12

[a]device performance based on 24 devices tested in each batch; P3HT was spin-coated at 700 rpm for 60 s; devices were thermally annealed at 150 °C for 10 min

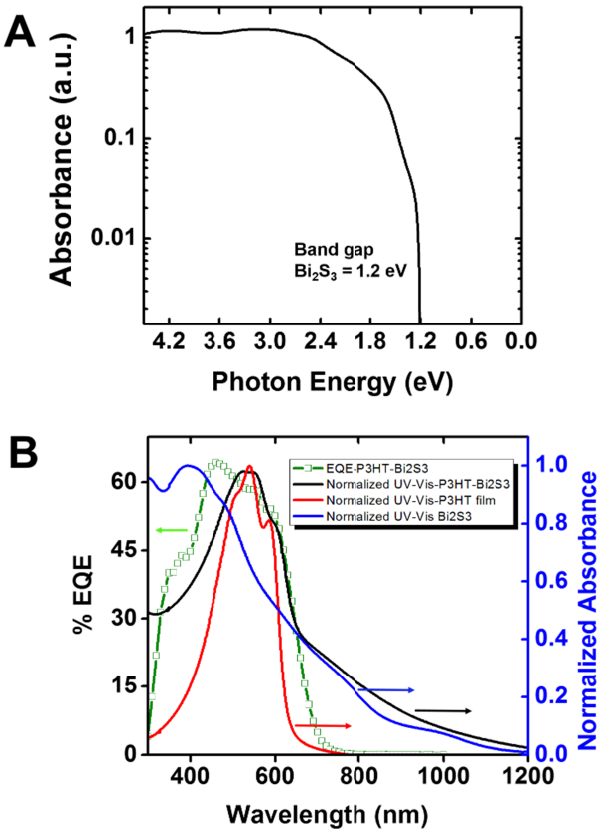

Figure S3. A) Absorption of Bi_2S_3 nanowire networks. From these measurements we calculated an optical bandgap of 1.2 eV for our Bi_2S_3 nanowire networks. B) EQE and UV-Vis data comparison for the individual constituents (Bi_2S_3 and P3HT) and P3HT-Bi_2S_3 active layers.

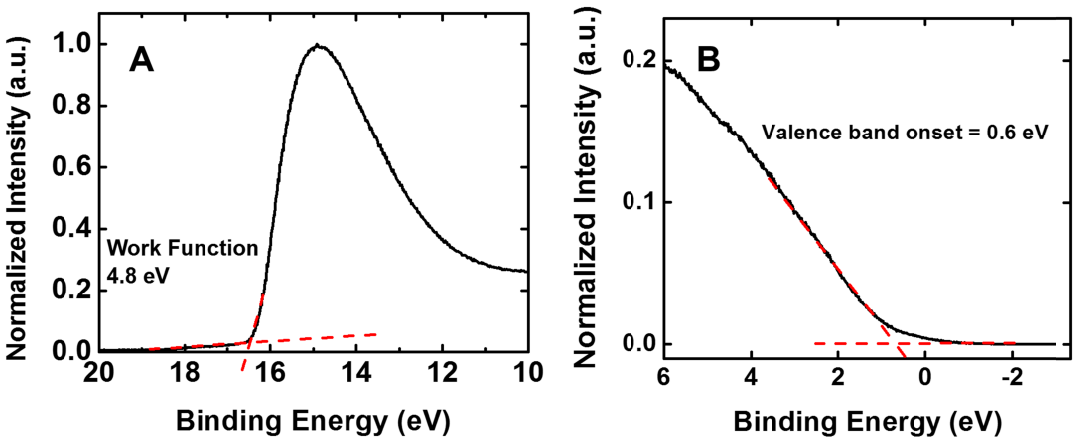

Figure S4. UPS spectra of Bi_2S_3 nanowire networks. A) secondary electron cutoff for work function determination. B) Magnification of the UPS spectra close to the Fermi level for the determination of the HOMO onset.

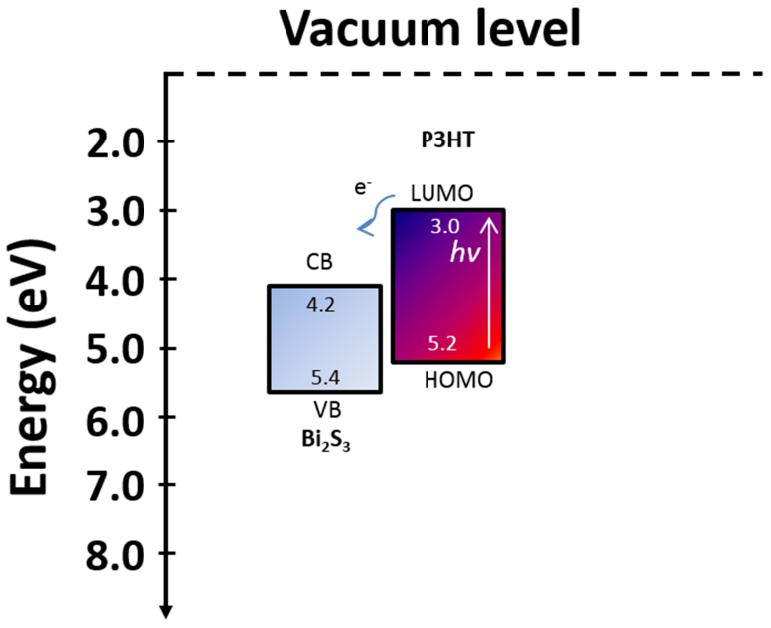

Figure S5. Energy diagram for Bi_2S3-P3HT active layers based on the energy levels of the individual constituents.

Figure S1 shows the morphological and structural characterization of as-synthesized Bi_2S_3 nanowires. From the SEM micrograph presented in **Figure S1A,** these nanowires are dimensionally uniform with an average length of 25 ± 5 μm and an average diameter of 30 ± 5 nm. **Figure S1B** shows the corresponding XRD pattern of the Bi_2S_3 nanowires, which provides definitive identification of the crystal structure of the nanowires. All the experimental reflections can be indexed to the Pbnm space group of Bi_2S_3 (Joint Committee of Powder Diffraction Standards (JCPDS) 17-0320).

The electrical transport measurements on a single nanowire allowed us to determine if our Bi_2S_3 nanowires are transporting holes or electrons. **Figure S2** shows the I_{DS}-V_G curve of a single-nanowire Bi_2S_3 field-effect transistor (FET) at room temperature under vacuum (10^{-5} torr). The device was measured at a fixed source-drain bias voltage of 2 V. The gate voltage was scanned from -10 V to +5 V. To compare the performance of this device with those reported in the literature, we calculated the field-effect mobility (μ) in the linear regime per equations below:[1]

$$\mu = g_m \times \frac{L}{C_t} \times \frac{1}{V_{DS}} \qquad \text{(S1)}$$

$$c_t = \frac{2\pi\varepsilon_{ox}}{\ln\left(\frac{4t_{ox}}{W}\right)} \qquad \text{(S2)}$$

where g_m is the transconductance, V_{DS} is the source-drain voltage, and L (520 nm) and W (30 nm) are the channel length and width of the Bi_2S_3 nanowire, respectively. C_t is the gate capacitance per unit length, where ε_{ox} is the dielectric constant of SiO_2 ($3.9\varepsilon_o$), and t_{ox} the SiO_2 thickness (300 nm). From the device characteristics in the linear regime, we calculated an electron mobility of 1.3 $cm^2V^{-1}s^{-1}$. The calculated mobility is on par with those reported in the literature for single-nanowire Bi_2S_3 devices.[2]

Table S1 shows the average and standard deviation values of performance characteristics for batches of hybrid devices comprising active layers having varying P3HT and Bi_2S_3 thicknesses. Subsequent device optimization and GIXD experiments were performed on the active layer that resulted in the highest performing devices, i.e., those having an active layer of 200 nm-thick Bi_2S_3 nanowire networks and 120 nm-thick P3HT layer.

Figure S3 shows the EQE and UV-Vis spectra for P3HT-Bi_2S_3 active layer as well as the neat components. From **Figure S3A**, we estimated an optical bandgap of 1.2 eV for our Bi_2S_3 nanowire networks. From the UV-Vis data presented in **Figure S3B,** we observe that our Bi_2S_3 nanostructures absorb strongly in the IR region. As such, we had originally believed that our Bi_2S_3 nanowire networks should contribute substantially to photocurrent generation beyond the visible region. While our EQE data does show some absorption beyond the absorption edge of P3HT, photocurrent generation does not extend to the IR nearly as much as the absorption of Bi_2S_3 suggests. We do, however, observe contribution to the EQE in the 400-500 nm range attributable to photoabsorption of Bi_2S_3.

We also calculated the work function of our percolated Bi_2S_3 networks from UPS measurements. From **Figure S4A**, we determined the work function of our Bi_2S_3 nanowire networks by extrapolating the cut-off energy values from the UPS spectrum. This extrapolation resulted in a work function value of 4.8 eV. The obtained work function value is comparable with values obtained for the work function of Bi_2S_3 quantum dots via kelvin probe force microscopy measurements.[3]

From the same UPS data, we calculated a valence band onset of 0.6 eV (**Figure S4B**), corresponding to a valence band level of 5.4 eV. Previously, Liao and coworkers reported the valence band (VB) and conduction band (CB) levels for Bi_2S_3 nanorods via cyclic voltammetry measurements.[4] By resolving the threshold point for the oxidation and reduction peaks obtained in their measurements, they obtained VB and CB edges of 5.2 eV and 3.8 eV, respectively. As such, the VB edge for our Bi_2S_3 nanowire networks obtained via UPS measurements is 0.2 eV higher than that reported by Liao and coworkers. This slight discrepancy might be related to the technique used to determine the energy levels of Bi_2S_3 nanostructures. It could also arise from differences in the dimensions and geometry of the nanostructures (dots as opposed to wires).

We constructed an energy diagram based on the experimentally obtained energy levels for Bi_2S_3 and published values for P3HT,[5-9] recognizing that this energy diagram does not account for band bending, the presence of interfacial dipoles or vacuum level shifts associated with interfacing Bi_2S_3 with P3HT. This energy diagram is presented in **Figure S5**.

References

1. W. M. Wang, M. C. LeMieux, S. Selvarasah, M. R. Dokmeci and Z. Bao, *ACS Nano*, 2009, **3**, 3543-3551.
2. K. Yao, Z. Y. Zhang, X. L. Liang, Q. Chen, L. M. Peng and Y. Yu, *J. Phys. Chem. B*, 2006, **110**, 21408-21411.
3. R. Narayanan, M. Deepa, F. Friebel and A. K. Srivastava, *Electrochim. Acta*, 2013, **105**, 599-611.
4. H.-C. Liao, M.-C. Wu, M.-H. Jao, C.-M. Chuang, Y.-F. Chen and W.-F. Su, *CrystEngComm*, 2012, **14**, 3645-3652.
5. B. C. Thompson and J. M. J. Fréchet, *Angew. Chem. Int. Edit.*, 2008, **47**, 58-77.
6. M. D. Irwin, D. B. Buchholz, A. W. Hains, R. P. H. Chang and T. J. Marks, *P. Natl. A. Sci.*, 2008, **105**, 2783-2787.
7. P. P. Khlyabich, B. Burkhart, A. E. Rudenko and B. C. Thompson, *Polymer*, 2013, **54**, 5267-5298.
8. Z.-L. Guan, J. Bok Kim, Y.-L. Loo and A. Kahn, *J. Appl. Phys.*, 2011, **110**, 043719/1-043719/4.
9. Z.-L. Guan, J. B. Kim, H. Wang, C. Jaye, D. A. Fischer, Y.-L. Loo and A. Kahn, *Org. Electron.*, 2010, **11**, 1779-1785.